Science
AAAS

The Genetic Architecture of Maize Flowering Time
Edward S. Buckler, *et al.*
Science **325**, 714 (2009);
DOI: 10.1126/science.1174276

ice-surface lowering or some regional climate change induced by ice-surface lowering. If attributed solely to a change in ice-surface elevation, the 3° to 4°C warming at Siple Dome (*16*) would indicate 500 to 650 m of ice-surface lowering, assuming a free atmospheric lapse rate of 6°C per 1000 m. This magnitude of lowering is supported by ice-sheet modeling, which suggests thinning of Siple Dome ice by 350 m between 14 and 15 ka (*17*). Within the large dating uncertainties of dated marine samples, widespread retreat of the Antarctic Peninsula Ice Sheet margin on the continental shelf also occurred at this time (*18*). These lines of direct evidence for WAIS retreat at the time of MWP-1A are consistent with geophysical modeling of the noneustatic component of the sea-level rise during MWP-1A, which suggests a dominant source from Antarctica (*19*).

15. E. J. Steig *et al*., *Science* **282**, 92 (1998).
16. E. J. Brook *et al*., *Quat. Sci. Rev.* **24**, 1333 (2005).
17. S. F. Price, H. Conway, E. D. Waddington, *J. Geophys. Res. Earth Surf.* **112**, F03021 (2007).
18. D. C. Heroy, J. B. Anderson, *Quat. Sci. Rev.* **26**, 3286 (2007).
19. S. E. Bassett, G. A. Milne, J. X. Mitrovica, P. U. Clark, *Science* **309**, 925 (2005).
20. Based on a larger data set, the mean age for regional deglaciation of mid-latitude Southern Hemisphere mountain glaciers (17.7 ka) is not significantly different from the previously reported mean age (17.3 ka), using the same scaling factor (*21*). Nevertheless, the age of regional deglaciation in the mid-latitude Southern Hemisphere is significantly younger than the regional deglaciation age established for LLGM glaciers at northern mid-latitudes (Fig. 3A), a finding counter to the conclusion that deglaciation in the two hemispheres was synchronous (*21*). The source of this disagreement appears to be that Schaefer *et al*. (*21*) identified "outer LGM" and "inner LGM" moraines in any given region, which in western North America are typically 20 to 21 ka and 16.5 to 17.5 ka, respectively (*22*). In these cases, and to be consistent with the concept of LLGM, we used the TCN ages of the "outer" moraines to mark the onset of regional deglaciation from the LLGM, whereas we viewed the "inner" moraines as recording a subsequent millennial-scale ice-margin fluctuation that is unrelated to the termination of the LLGM.
21. J. M. Schaefer *et al*., *Science* **312**, 1510 (2006).
22. J. M. Licciardi, P. U. Clark, E. J. Brook, D. Elmore, P. Sharma, *Geology* **32**, 81 (2004).
23. Heinrich event 2 (H2), which occurred during the LGM ~24 ka, is generally thought to represent an instability of the LIS. In either case, we view H2 as an anomalous and short-lived event with respect to the 7500-year-long LGM interval, during which time ice sheets were otherwise largely in equilibrium with climate.
24. A. J. Weaver, O. Saenko, P. U. Clark, J. X. Mitrovica, *Science* **299**, 1709 (2003).
25. L. C. Skinner, N. J. Shackleton, *Quat. Sci. Rev.* **24**, 571 (2005).
26. C. Waelbroeck *et al*., *Quat. Sci. Rev.* **21**, 295 (2002).
27. D. P. Schrag, G. Hampt, D. W. Murray, *Science* **272**, 1930 (1996).
28. L. Lisiecki, M. E. Raymo, *Paleoceanography* **20**, PA1003 (2005).
29. R. Bintanja, R. S. W. van de Wal, *Nature* **454**, 869 (2008).
30. S. Levitus, *World Ocean Atlas 1994* (U.S. Government Printing Office, Washington, DC, 1994).
31. D. W. Lea, D. K. Pak, H. J. Spero, *Science* **289**, 1719 (2000).
32. J. Imbrie *et al*., *Paleoceanography* **8**, 699 (1993).
33. P. Huybers, *Science* **313**, 508 (2006).
34. M. Feldberg, A. C. Mix, *Paleoceanography* **18**, 10.1029/2001PA000740 (2003).
35. I. Martinez, L. Keigwin, T. T. Barrows, Y. Yokoyama, J. Southon, *Paleoceanography* **18**, PA000877 (2003).
36. L. Stott, C. Poulsen, S. Lund, R. Thunell, *Science* **297**, 222 (2002).
37. A. C. Clement, R. Seager, M. A. Cane, *Paleoceanography* **14**, 441 (1999).
38. P. U. Clark, S. W. Hostetler, N. G. Pisias, A. Schmittner, K. J. Meisner, in *Ocean Circulation: Mechanisms and Impacts*, A. Schmittner, J. Chiang, S. Hemming, Eds. (Geophysical Monograph 173, American Geophysical Union, Washington, DC, 2007), pp. 209–246.
39. To estimate this mass increase, we used the area of the LIS at 13 ka (7.35×10^6 km^2) multiplied by the mass balance increase of 0.17 m year^{-1} over 6500 years, resulting in 24 m of sea-level equivalent. The LIS expanded to its LGM area of 11.63×10^6 km^2 over 6500 years, resulting in an average annual rate of area increase of 611 km^2 year^{-1}. The assumption that the mass balance increase of 0.17 m year^{-1} applied to this expanding area over 6500 years results in an additional 7 m of sea-level equivalent.
40. L. Stott, A. Timmermann, R. Thunell, *Science* **318**, 435 (2007).
41. P. Huybers, G. Denton, *Nat. Geosci.* **1**, 787 (2008).
42. P. U. Clark, R. B. Alley, D. Pollard, *Science* **286**, 1104 (1999).
43. J. C. H. Chiang, C. M. Bitz, *Clim. Dyn.* **25**, 477 (2005).
44. A. B. G. Bush, S. G. H. Philander, *Science* **279**, 1341 (1998).
45. We examined the possibility that the perturbation to the threshold in summer energy (τ) due to LGM boundary conditions (*7*) may have induced a summer energy budget that favored mountain glaciation LLGM at times other than the LGM, but this did not prove to be the case.
46. A. S. Dyke, V. K. Prest, *Geogr. Phys. Quat.* **XLI**, 237 (1987).
47. J. P. Briner, G. H. Miller, P. T. Davis, R. C. Finkel, *Can. J. Earth Sci.* **42**, 67 (2005).
48. K. Pahnke, R. Zahn, H. Elderfield, M. Schulz, *Science* **301**, 948 (2003).
49. T. Blunier, E. J. Brook, *Science* **291**, 109 (2001).
50. Y. J. Wang *et al*., *Science* **294**, 2345 (2001).
51. W. R. Peltier, *Annu. Rev. Earth Planet. Sci.* **32**, 111 (2004).
52. R. L. Edwards *et al*., *Science* **260**, 962 (1993).
53. J. Chappell, *Quat. Sci. Rev.* **21**, 1229 (2002).
54. E. Bard, B. Hamelin, R. G. Fairbanks, A. Zindler, *Nature* **345**, 405 (1990).
55. T. Hanebuth, K. Stattegger, P. M. Grootes, *Science* **288**, 1033 (2000).
56. A. C. Mix *et al*., in *Mechanisms of Global Climate Change at Millennial Time Scales*, P. U. Clark, R. S. Webb, L. D. Keigwin, Eds. (Geophysical Monograph 112, American Geophysical Union, Washington, DC, 1999), pp. 127–148.
57. N. J. Shackleton, M. A. Hall, E. Vincent, *Paleoceanography* **15**, 565 (2000).
58. J. Laskar, P. Robutel, M. Gastineau, A. C. M. Correia, B. Levrard, *Astron. Astrophys.* **428**, 261 (2004).
59. J. Ahn *et al*., *J. Geophys. Res.* **109**, D13305 (2004).
60. J. Ahn, E. J. Brook, *Science* **322**, 83 (2008).
61. A. Svensson *et al*., *Clim. Past* **4**, 47 (2008).
62. The authors thank J. Licciardi, N. Pisias, and an anonymous reviewer for their constructive comments, and J. Bockheim, B. Hall, and P. Huybers for discussions. This work was supported by NSF (P.U.C., J.D.S., A.E.C., and S.W.H.), the Geological Survey of Canada Climate Change Program (A.S.D.), the University of Wisconsin (A.E.C.), the Swedish Nuclear Fuel and Waste Management Co. (B.W.), and the Canadian Institute for Advanced Research (J.X.M.).

Supporting Online Material

www.sciencemag.org/cgi/content/full/325/5941/710/DC1
Materials and Methods
SOM Text
Figs. S1 to S5
References

27 February 2009; accepted 23 June 2009
10.1126/science.1172873

The Genetic Architecture of Maize Flowering Time

Edward S. Buckler,[1,2,3]* James B. Holland,[1,4]* Peter J. Bradbury,[1,2] Charlotte B. Acharya,[2] Patrick J. Brown,[2] Chris Browne,[1,5] Elhan Ersoz,[2] Sherry Flint-Garcia,[1,5] Arturo Garcia,[1,5] Jeffrey C. Glaubitz,[6] Major M. Goodman,[4] Carlos Harjes,[7] Kate Guill,[1,5] Dallas E. Kroon,[2] Sara Larsson,[3] Nicholas K. Lepak,[1,3] Huihui Li,[8,2,9] Sharon E. Mitchell,[2] Gael Pressoir,[2] Jason A. Peiffer,[3] Marco Oropeza Rosas,[4] Torbert R. Rocheford,[10,11] M. Cinta Romay,[2,12] Susan Romero,[2] Stella Salvo,[1,4] Hector Sanchez Villeda,[5,13] H. Sofia da Silva,[10] Qi Sun,[14] Feng Tian,[2] Narasimham Upadyayula,[10] Doreen Ware,[1,15] Heather Yates,[2] Jianming Yu,[16] Zhiwu Zhang,[2] Stephen Kresovich,[2]* Michael D. McMullen[1,5]*

Flowering time is a complex trait that controls adaptation of plants to their local environment in the outcrossing species *Zea mays* (maize). We dissected variation for flowering time with a set of 5000 recombinant inbred lines (maize Nested Association Mapping population, NAM). Nearly a million plants were assayed in eight environments but showed no evidence for any single large-effect quantitative trait loci (QTLs). Instead, we identified evidence for numerous small-effect QTLs shared among families; however, allelic effects differ across founder lines. We identified no individual QTLs at which allelic effects are determined by geographic origin or large effects for epistasis or environmental interactions. Thus, a simple additive model accurately predicts flowering time for maize, in contrast to the genetic architecture observed in the selfing plant species rice and *Arabidopsis*.

The nature of standing genetic variation and its relation to phenotypic variation in plants affects our understanding of evolution (*1*), sustainable agriculture, and preservation of inter- and intraspecific variation in times of environmental change. Maize inbred lines have an average nucleotide diversity in genic regions around 1% (π = 1 to 1.4%) (*2*, *3*),

similar to the divergence between humans and chimpanzees (*4*). It is not uncommon to find maize haplotypes that are 5% divergent from one another (*5*), which indicates that the maize gene pool reaches back 2 to 4 million years (with one generation per year).

Maize is adapted to a range of environments from the lowland tropics to the Andean highlands and has been widely introduced worldwide into both temperate and tropical regions. Maize's genetic architecture for flowering time has evolved as its wild relatives adapted to distinct ecological zones in elevations differing by more than 3000 m in Mexico and then under both natural and artificial selection over the last 7000 years, with especially intense selection over the past century. This genetic architecture has evolved under a predominantly outcrossing mating system in a species with little population differentiation (*6*).

Flowering time reflects the adaptation of a plant to its environment by tailoring vegetative and reproductive growth phases to local climatic effects. Maize landraces vary widely, from 2 to 11 months, for the time required to mature (*7*). In addition, asynchrony of male and female flowering in maize may be adaptive in some cultivars, but can result in losses under drought conditions, especially in modern uniform varieties (*8*). Flowering time has been extensively studied in the predominantly self-fertilizing species *Arabidopsis*. Like maize, *Arabidopsis* grows across a wide range of latitudes and has flowering time controlled by the interaction of the photoperiod (light sensing and circadian rhythm), vernalization, and autonomous flowering and gibberellic acid–response pathways (*9*, *10*). In grasses, which include maize, wheat, and rice, some of the same genes are involved in flowering, but they have different functions (*11*–*13*).

In maize, diversity-based dissection of flowering time has been hindered by tight linkage of the trait to population structure and by the lack of a reference genome. However, putative orthologs for flowering-time genes identified in other species have been identified through QTL meta-analyses (*14*), although only one major maize flowering-time QTL has been positionally cloned [*vegetative to generative transition 1* (*vgt1*) (*15*)].

Experimental design. We used the maize NAM population (*16*) of 200 recombinant inbred lines (RILs) from 25 crosses between diverse inbred lines and B73 (each referred to as a family), which resulted in a total of 5000 lines (*17*). Because maize has rapid linkage disequilibrium (LD) decay, joint linkage analysis of the maize NAM population was used to evaluate complex trait genetic architecture, as we have insufficient marker density for a genome-wide association study (GWAS). The 5000 lines plus 500 checks—nearly one million plants—were evaluated in four locations over 2 years. We scored days to silking (DS, female flowering) and days to anthesis (DA, male flowering), and we calculated the anthesis-silking interval (ASI). We estimated heritability to be 94% for DS and DA and 78% for ASI; within-cross heritability averaged 83 to 84% for DS and DA and 68% for ASI (table S1). Overall, our phenotypic data were highly heritable, and substantial replication across environments reduced environmental effects on the phenotypic mean values of the lines.

Genetic architecture of flowering. We mapped QTLs both within the 25 families separately (using stepwise regression and inclusive composite interval mapping) and in joint analyses that combined information across all families (joint stepwise regression and joint inclusive composite interval mapping, JICIM (*17*). These methods produced concordant results in terms of the magnitude of effects; however, they have different power and resolution capabilities. Joint linkage QTL analysis identifies nearly twice as many significant effects compared with individual family analyses. The multiple-family joint stepwise regression method identified 36 and 39 QTLs that explained 89% of the total variance for DA or DS, respectively, whereas 29 QTLs explained 64% of the ASI variance (Fig. 1, top). JICIM generally found evidence for an additional 20 minor QTLs for each trait (Fig. 1, bottom). These findings are concordant with the evidence for 50 or more QTLs identified that affect oil content in a large maize population (*18*). Six major QTL regions previously identified in meta-analysis of maize flowering (*14*) were concordant with QTLs identified here. Robust QTL mapping with NAM permitted unprecedented estimation of the genetic architecture in terms of the magnitude of gene effects, epistasis, gene-environment interactions, and pleiotropy.

The number of days to silk emergence varied by 32 days among NAM founder lines and by 28 days among NAM RILs. However, relative to B73, the largest effect DS QTL allele had an additive effect of only 1.7 days (Fig. 2A), whereas the largest ASI effect was 0.4 days. Over 98% of the QTL alleles affected DS by less than 1 day (Fig. 2A). In contrast, in *Arabidopsis*, crosses between lines that flower at roughly the same time can segregate for QTLs that have 3- to 18-day effects (*19*). Rice and barley, both self-fertilizing species, also exhibit larger additive effects for variation in flowering time (*20*, *21*). *Ma1*, the major photoperiod-sensitivity locus in sorghum, has an additive effect of 40.3 days and explains 85.7% of the phenotypic variance for flowering time in a close interspecific (*Sorghum bicolor* × *S. propinquum*) mapping family (*22*).

Our results demonstrate that large differences in flowering time among inbred maize lines are not caused by a few genes of large effect, but by the cumulative effects of numerous QTLs (Fig. 2B), each with only a small impact on the trait. The latest flowering lines had significant allele effects at 24 QTLs, of which 75% delay flowering; the earliest had significant allele effects at 18 QTLs, with 66% of the QTLs accelerating flowering. In outbreeding species, flowering of individual plants must be substantially synchronous within a local population to ensure mating success. Selection may have favored a genetic architecture of additive small-effect QTLs, so that most offspring are likely to have partially synchronous flowering times to ensure fitness. The dispersion of heritable effects across 50 to 100 of these small-effect QTLs may permit the adaptation to a wide range of environments by accumulation of alleles that consistently increase or decrease flowering time.

We tested all pairwise marker combinations for epistatic interactions within each family separately. Epistatic interactions were detected for DS and DA and only within two families. We also tested all marker pairs for epistasis in a joint analysis of all populations, which resulted in detection of epistasis for two marker pairs for ASI, which, combined, explained only 2% of the phenotypic variation. The low epistasis detected for these traits was surprising because flowering time in plants results from interactive molecular pathways (*10*), and epistatic effects have been observed in *Arabidopsis* (*23*) and rice (*24*).

In general, the vast majority of flowering QTLs we identified showed largely consistent results across environments. Although 59% of QTLs had significant environmental (E) interactions, the genetic variation was many times larger than QTL×E interaction variation (Fig. 3A). Overall, this suggests a stable genetic architecture across environments. ASI appeared more sensitive to genotype-by-environment interactions (G×E) than the other flowering phenotypes observed here. Our testing environments had substantial differences in temperatures and rainfall, but day lengths were consistently longer than the critical photoperiod for short-day maize. Therefore, we

[1]U.S. Department of Agriculture (USDA)–Agricultural Research Service (USDA-ARS). [2]Institute for Genomic Diversity, Cornell University, Ithaca, NY 14853, USA. [3]Department of Plant Breeding and Genetics, Cornell University, Ithaca, NY 14853, USA. [4]Department of Crop Science, North Carolina State University, Raleigh, NC 27695, USA. [5]Division of Plant Sciences, University of Missouri, Columbia, MO 65211, USA. [6]Laboratory of Genetics, University of Wisconsin, Madison, WI 53706, USA. [7]Monsanto Company, Leesburg, GA 31763, USA. [8]School of Mathematical Science, Beijing Normal University, Beijing 100875, China. [9]Institute of Crop Science, Chinese Academy of Agricultural Sciences, Beijing 100081, China. [10]Department of Crop Sciences, University of Illinois, Urbana, IL 61801, USA. [11]Department of Agronomy, Purdue University, Urbana, IL 61801, USA. [12]Mision Biologica de Galicia, (CSIC), Pontevedra 36080, Spain. [13]CIMMYT, INT, Crop Research Laboratory, Carretera Mex-Veracruz, CP 56130, Mexico. [14]Computational Biology Service Unit, Cornell University, Ithaca, NY 14853, USA. [15]Cold Spring Harbor Laboratory, Cold Spring Harbor, NY 11724, USA. [16]Department of Agronomy, Kansas State University, Manhattan, KS 66506, USA.

*To whom correspondence should be addressed. E-mail: esb33@cornell.edu (E.S.B.); james_holland@ncsu.edu (J.B.H.); sk20@cornell.edu (S.K.); mcmullenm@missouri.edu (M.D.M.)

expect that G×E interactions may be stronger if tested under both short and long day length environments.

This study was able to investigate pleiotropy by correlating the allelic effects on multiple traits of each QTL across a robust sample of founders. We observed that 100% of DS and DA QTLs have correlated effects on both male and female flowering (average $r = 0.90$ across all loci). In contrast, only about 70% of ASI QTLs had correlated effects on DS, and only 14 to 21% of the ASI QTLs had correlated effects on DA. Overall, genetic control of male and female flowers appears to involve the same set of genes (although magnitudes of effects likely vary). However, the asymmetry between DA-ASI and DS-ASI correlations resulted from the higher variation in the DS phenotype.

We used the significant NAM QTL additive effect estimates to predict the timing of flowering of the NAM founder lines and were able to accurately predict parental flowering time (R^2 = 87 to 91%) (Fig. 3B). This suggests that NAM QTL results are more reliable than individual family QTL effect estimates (*25*) and provides further evidence that epistasis is relatively unimportant. By including nonsignificant additive effect estimates in the model, analogous to genome selection, our predictive ability increases to R^2 = 95%. Although we cannot extend these predictions to unrelated lines because of insufficient marker density, our results suggest that with large enough samples, additive QTL models can accurately predict phenotype.

Our maize founder lines represent a wide range of latitudinal variation (tropical ↔ temperate dent ↔ Northern Flint). We tested the correlation between QTL effect estimates of each founder allele with quantitative estimates of their relation to families of origin to determine whether population structure is defined by the allelic effects at any individual QTL (*26*). QTL effects at 26% of the loci were correlated ($P < 0.05$) with the tropical-temperate cline. The large effects observed for the QTLs on chromosome 10 were highly correlated with tropical origin, yet only 3 of the 16 lines with substantial tropical origin carried alleles at this locus that increased time to flowering by more than 0.4 days. Overall, allelic effects at many loci were weakly correlated with population structure, but tropical origin was not defined by specific QTL alleles; instead, it appears that numerous loci work in concert to produce latitudinal adaptations (Fig. 4A).

QTL and allele frequency. Thirty percent of the polymorphisms in maize were found to be unique to a single founder line (Fig. 4B), which indicates that rare sequence variants are common in diverse maize. We tested whether the phenotypic variation observed across families was mostly due to many rare variants (segregating in only one family) or to a smaller number of loci causing variation in multiple families. As each founder line gave rise to 200 offspring RILs, represented by about 40,000 plants, our design provided sufficient power to detect rare QTLs and to distinguish between these alternative

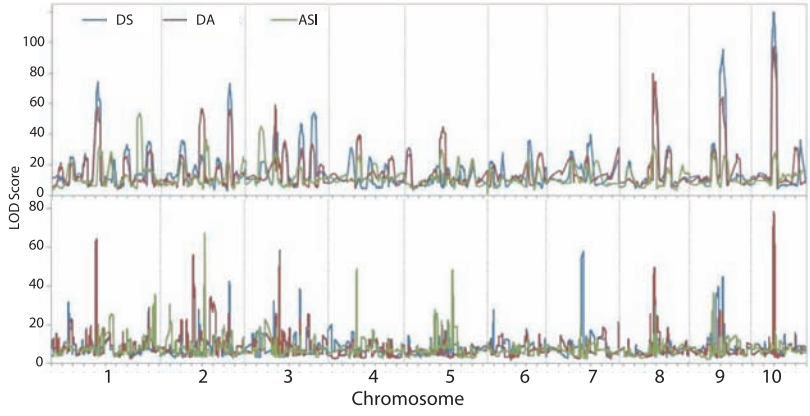

Fig. 1. Joint QTL mapping results across the genome for DS, DA, and ASI. The vertical lines indicate the breaks between the chromosomes. (**Top**) Scanning of the whole genome by using the joint General Linear Model (GLM). (**Bottom**) The whole genome scanned by JICIM.

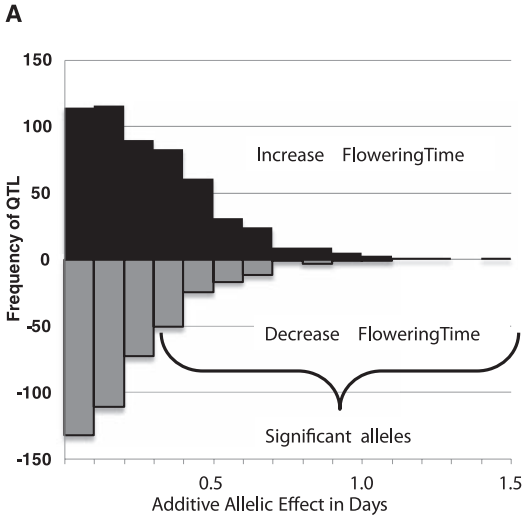

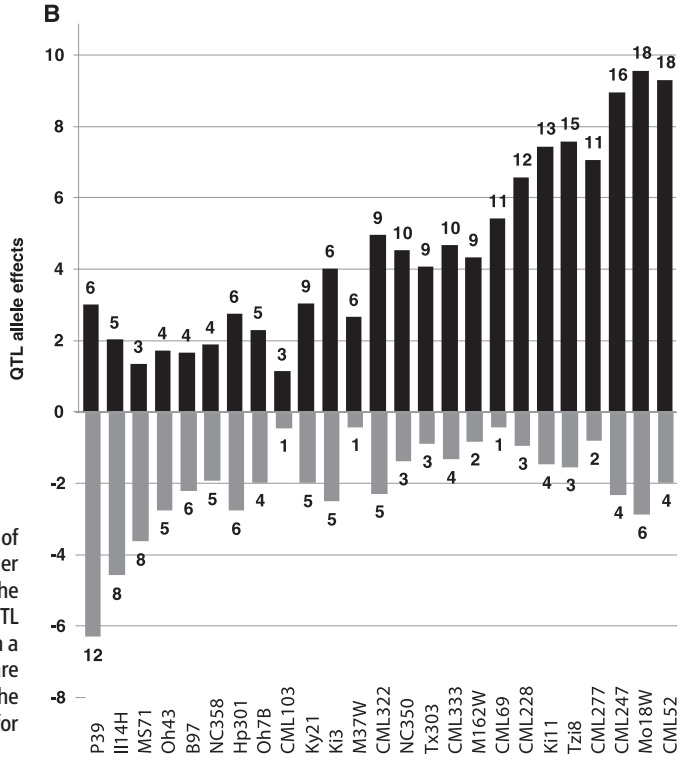

Fig. 2. All QTL allele effects were relatively modest. (**A**) Histogram of additive allele estimates for the 39 days to silking QTLs for all 25 founder lines relative to B73. Count of effects increasing flowering time above the line, and decreasing flowering time below the line. There were 333 QTL alleles that were significant at $P < 0.05$. Only seven (2.1%) had more than a 1-day effect on flowering time. (**B**) Large differences in the parental lines are the product of stacking large numbers of modest-effect QTL. Sums of the estimated additive positive and negative QTL allele effects for each line for DS. Number of QTLs next to each bar.

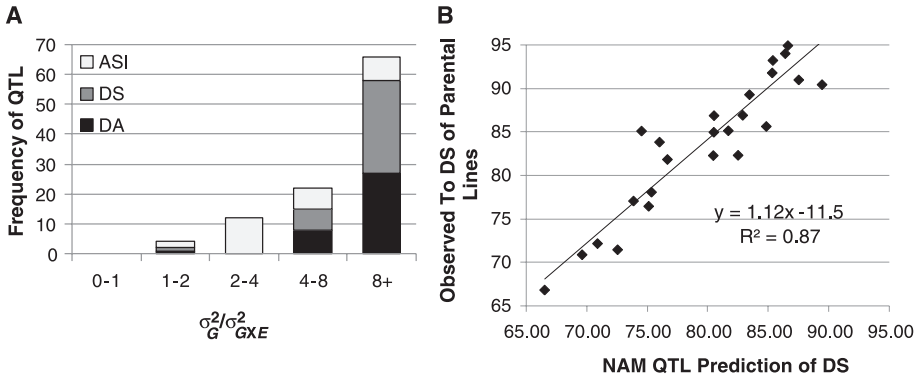

Fig. 3. (**A**) Ratio of genetic variance to genotype by environmental variance by trait. All traits were dominated by genetic variance, but Q×E was more important for ASI. (**B**) Parental flowering can be predicted well from the NAM QTL estimates. All significant QTL effects ($P < 0.05$) for DS were summed and added to observed B73 flowering to predict parental flowering. A consistent underestimate of the slope is likely because of epistasis. The fit increased when nonsignificant alleles were included to $R^2 = 0.95$.

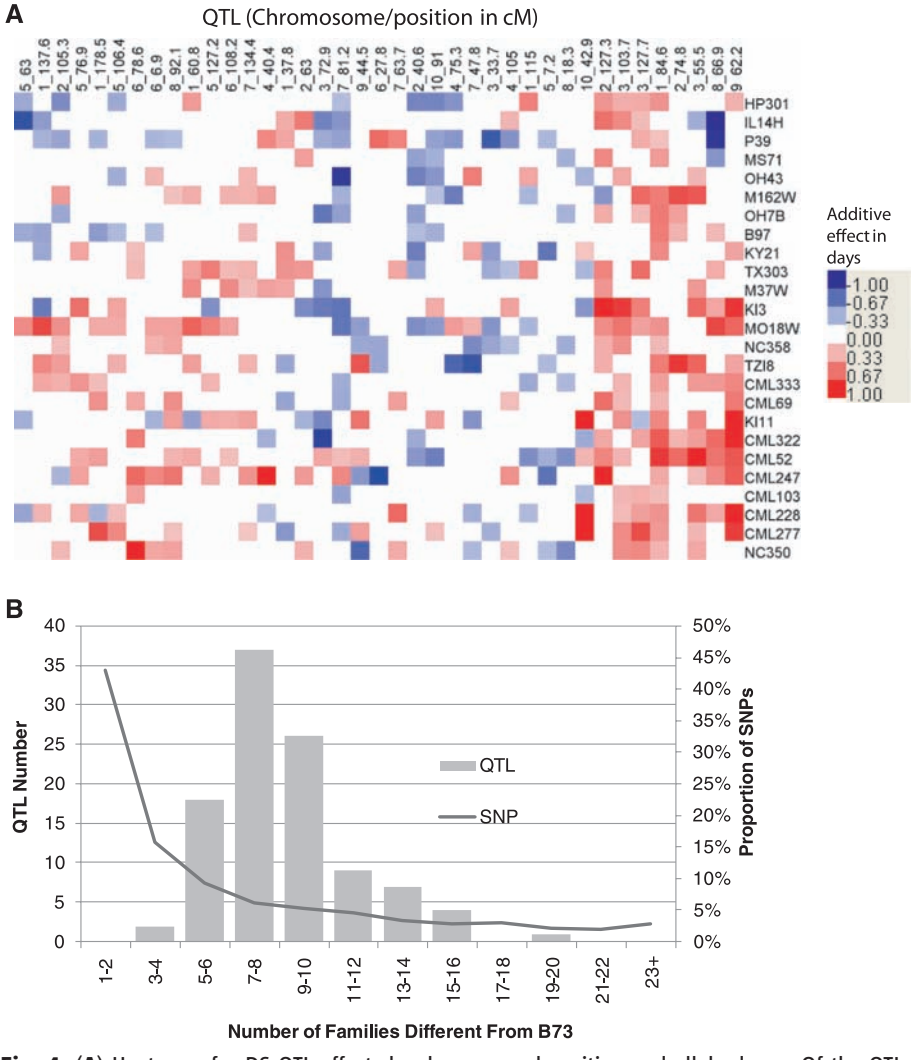

Fig. 4. (**A**) Heat map for DS QTL effects by chromosomal position and allele donor. Of the QTLs, 69% had both positive and negative effects relative to B73, which suggests that allelic series are important for maize flowering-time variation. The QTLs and population were clustered and sorted to show maximal population differentiation of QTLs and lines. Although some QTLs certainly are more common in tropical or temperate lines, no QTL sharply defined these differences. (**B**) The distribution of QTLs and SNPs across families was extremely different, with biases toward QTLs of intermediate frequencies. The QTL and SNP frequency among the NAM families for the three combined traits (DA, DS, and ASI) showed similar distributions. The SNP line indicates the observed frequency of SNP differences from a set 3641 SNPs identified through sequencing these lines.

hypotheses (>90% power for 1-day effect even in single-family analysis). Most QTLs were shared among multiple families (Fig. 4B), with many QTLs showing effects among seven to eight families (30% frequency). Our data partially support the common gene hypothesis for flowering-time genetic architecture, which proposes that variation at common loci causes phenotypic variation across different families. This result is striking because the sharing of QTLs across families contrasts with the high frequency of rare single-nucleotide polymorphisms (SNPs) in maize (Fig. 4B). This discrepancy cannot be due to bias in detecting QTLs of modest frequency for several reasons. (i) Although lower than that for common QTLs, our design provides enough power to detect QTLs segregating in two to four families; nevertheless, we observed few QTLs distributed in this way. (ii) NAM can statistically detect QTLs unique to B73 (common QTLs in this reference design, but rare QTL alleles in the species). However, only 1% of the QTLs were found in 17 or more families compared with 10% of the SNPs. (iii) Additional QTLs can be identified within individual families, but when they were added to the joint family analysis models, they showed significant effects in additional families. And (iv), retesting the final joint population QTLs model by jackknifing the families (leaving one or two families out sequentially) resulted in reduced significance for some of the QTLs, but none became insignificant.

Although many QTLs appear to be shared across families, we also found evidence for allelic series at most loci. Because our founders were crossed to a common reference line, we tested for and observed allelic series, including both positive and negative effects, at the same locus for 69 to 72% of the QTLs (Fig. 4A), depending on the trait. Such allelic series have previously been observed in maize (*27*). Although rare alleles dispersed across multiple tightly linked QTLs may also be misclassified as an allelic series in some cases, our association analysis suggests an allelic series for flowering-time effects at *vgt1* (below). Our results suggest a model of common genes with uncommon variants controlling flowering to explain our observation of a relatively small number of QTLs (e.g., <100), with many functionally distinct alleles at each locus, each occurring at low frequency. GWAS studies and fine-mapping multiple alleles per QTL will be needed to test this hypothesis.

Genes underlying this architecture. To evaluate the power and reliability of NAM, we

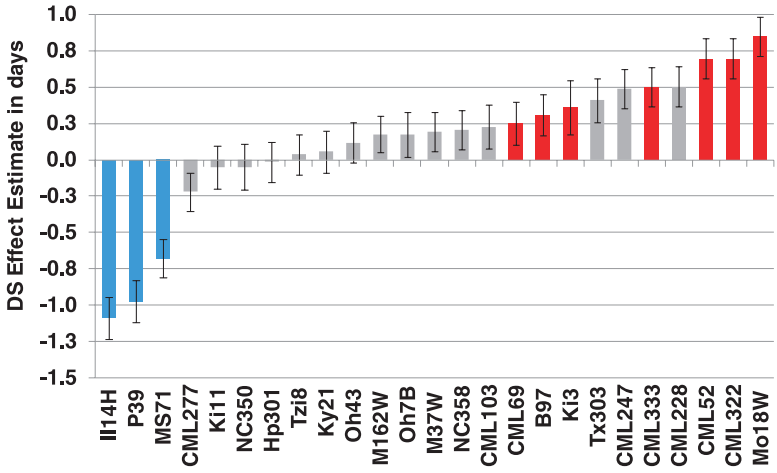

Fig. 5. Estimated DS effects and standard errors for the *vgt1* region of chromosome 8. Estimates are relative to B73 allele flowering. The blue alleles have the MITE at *vgt1* (the Mo17 family, also scored at the same time, also carries the polymorphism and equivalent effect). A simple *t* test of founder-effect estimate for MITE versus non-MITE was significant ($P = 2 \times 10^{-8}$). The red alleles identify lines that carry polymorphisms at *vgt1* target gene *rap2.7,* which also differs significantly ($P = 6 \times 10^{-4}$).

tested a QTL previously shown to affect flowering time in maize. The maize *vgt1* locus contains an *AP2*-like gene, *rap2.7*, involved in the timing of flowering under regulatory control of an enhancer region about 70 kb from the gene (*15*). We confirmed the presence of a QTL in the region of *vgt1* (DA: $P = 4 \times 10^{-44}$; DS: $P = 7 \times 10^{-40}$). Prior QTL mapping efforts (*28*) revealed an early flowering QTL about 5 centimorgans (cM) from *vgt1* that also may be contributing to the effects detected in this region; marker saturation across this interval permitted resolution into two linked QTLs. By controlling for the rest of the genome and estimating the effects of founder alleles at *vgt1*, we observed a distinct allelic series at this locus (Fig. 5).

A previously identified *vgt1* allele from northern germplasm associated with a miniature transposon (MITE) (*15*) was segregating in four of the NAM families (crosses involving Il14H, P39, MS71, and Mo17). In confirmation of previous results, this allele was strongly associated with early flowering in NAM (Fig. 5). Absence of this MITE did not explain the late flowering *vgt1* alleles, but sequencing of founder lines in this region identified SNPs at the *rap2.7* gene itself that were associated with this late-flowering effect (Fig. 5). Associations of both the MITE at the upstream regulator region (*vgt1*) and the SNPs within the *rap2.7* gene with flowering time were confirmed in a separate diverse maize inbred association panel (MITE: $P = 6 \times 10^{-4}$; *rap2.7* SNP: $P = 0.01$).

Natural variation at the *zfl2* locus also significantly affects flowering time (*29*). Although the null mutants of this gene previously observed in natural populations (*29*) did not segregate among these NAM families, we nevertheless found a QTL at the *zfl2* locus (DA: $P = 3 \times 10^{-10}$; DS: $P = 1 \times 10^{-15}$). One line, Ky21, had a phenotype associated with a 16–amino acid deletion in the proline-rich domain of this protein. In addition, other lines showing large effects have a 7-bp deletion 1 bp before the ATG start site of *zfl2*.

Marker saturation of RILs with recombinant chromosome blocks around the largest-effect QTL on chromosome 1 resolved the QTL to a region that includes a homolog of the recently cloned *Ghd7* gene from rice (*12*). On chromosome 1, the *bif2* gene, which is involved in auxin transport (*30*), overlaps with a QTL for ASI. Association analysis in unrelated lines implicates *bif2* in the timing of flowering (*31*). In addition, maize flowering mutant *id1* and homologs of the barley photoperiod genes (*Ppd-H1*) (*21*) fall within our QTL intervals. As there are over 1000 homologs of *Arabidopsis* flowering-time genes in maize, our study demonstrates a means by which to reliably relate maize QTLs to candidate genes.

Implications. Our study of QTLs controlling flowering time with NAM provides insight into the genetic architecture of adaptive traits. Our results suggest that for the outcrossing species maize, the genetic architecture of flowering time is dominated by small additive QTLs with few genetic or environmental interactions (within the tested range of environments). Human height may have a similar genetic architecture (*32*), but in the case of flowering time, these architectures are distinct from *Arabidopsis* and rice, self-fertilizing plant species, where flowering-time variation is controlled by fewer genes with larger effects, epistasis, and environmental interactions (*9*, *11*, *13*, *23*). This suggests that the mating system and demographics influence the genetic architecture of adaptive traits.

For maize, we now have some of the best genetic tools to conduct research of complex genetic architectures. We currently have nearly 15,000 genetic stocks for manipulation and isolation of the genetic variation throughout the entire species. We predict that soon it will be possible to more fully examine the genetic architecture of other traits of interest in maize. Such studies can be applied to improving the world's food security and to making maize production more environmentally sustainable.

References and Notes

1. T. Mitchell-Olds, J. Schmitt, *Nature* **441**, 947 (2006).
2. M. I. Tenaillon *et al.*, *Proc. Natl. Acad. Sci. U.S.A.* **98**, 9161 (2001).
3. S. I. Wright *et al.*, *Science* **308**, 1310 (2005).
4. The Chimpanzee Sequencing and Analysis Consortium, *Nature* **437**, 69 (2005).
5. A. M. Henry, C. Damerval, *Mol. Gen. Genet.* **256**, 147 (1997).
6. M. T. Hamblin, M. L. Warburton, E. S. Buckler, *PLoS One* **2**, e1367 (2007).
7. N. N. Kuleshov, *J. Am. Soc. Agron.* **25**, 688 (1933).
8. J. Bolanos, G. O. Edmeades, *Field Crops Res.* **48**, 65 (1996).
9. T. Izawa, Y. Takahashi, M. Yano, *Curr. Opin. Plant Biol.* **6**, 113 (2003).
10. Y. Komeda, *Annu. Rev. Plant Biol.* **55**, 521 (2004).
11. M. Yano, T. Izawa, in *Rice Genetics V: Proceedings of the Fifth International Rice Genetics Symposium*, 19 to 23 November 2005, Manila, Philippines (IRRI, World Scientific, Singapore, 2005), pp. 177–190.
12. W. Xue *et al.*, *Nat. Genet.* **40**, 761 (2008).
13. J. Cockram *et al.*, *J. Exp. Bot.* **58**, 1231 (2007).
14. F. Chardon *et al.*, *Genetics* **168**, 2169 (2004).
15. S. Salvi *et al.*, *Proc. Natl. Acad. Sci. U.S.A.* **104**, 11376 (2007).
16. M. D. McMullen *et al.*, *Science* **325**, 737 (2009).
17. Materials and methods are available as supporting material on *Science* Online.
18. C. C. Laurie *et al.*, *Genetics* **168**, 2141 (2004).
19. C. Alonso-Blanco, S. E. El-Assal, G. Coupland, M. Koornneef, *Genetics* **149**, 749 (1998).
20. M. Yano *et al.*, *Theor. Appl. Genet.* **95**, 1025 (1997).
21. A. Turner, J. Beales, S. Faure, R. P. Dunford, D. A. Laurie, *Science* **310**, 1031 (2005).
22. Y. R. Lin, K. F. Schertz, A. H. Paterson, *Genetics* **141**, 391 (1995).
23. M. E. El-Lithy *et al.*, *Genetics* **172**, 1867 (2006).
24. N. Uwatoko *et al.*, *Euphytica* **163**, 167 (2008).
25. C. C. Schon *et al.*, *Genetics* **167**, 485 (2004).
26. K. Liu *et al.*, *Genetics* **165**, 2117 (2003).
27. C. E. Harjes *et al.*, *Science* **319**, 330 (2008).
28. S. Salvi *et al.*, *Plant Mol. Biol.* **48**, 601 (2002).
29. K. Bomblies, J. F. Doebley, *Genetics* **172**, 519 (2006).
30. P. McSteen *et al.*, *Plant Physiol.* **144**, 1000 (2007).
31. G. Pressoir *et al.*, *Plant J.* **58**, 618 (2009).
32. P. M. Visscher, *Nat. Genet.* **40**, 489 (2008).

33. We thank the Buckler, Holland, Kresovich, McMullen, and Rocheford labs for their efforts in creating the populations, phenotyping the lines, and scientific input; L. R. Lirette for technical editing of the manuscript; and J. Doebley for managing the NSF project. This work was supported by U.S. NSF Plant Genome Program (DBI-9872631, DBI-0321467, DBI-0820619 to E.S.B., M.M.G. (98,03), J.B.H. (03,08), M.D.M. (03,08), S.K. (03,08), D.W. (03); DBI-0604923 to T.R.R.; U.S. Department of Agriculture–Agricultural Research Service (to E.S.B., J.B.H., M.D.M.), and Spanish Ministry for Education and Science (AP-2004-6033, fellowship to M.C.R.).

Supporting Online Material

www.sciencemag.org/cgi/content/full/325/5941/714/DC1
Materials and Methods
Tables S1 to S5
References

31 March 2009; accepted 26 June 2009
10.1126/science.1174276